Pakistan Veterinary Journal

ISSN: 0253-8318 (PRINT), 2074-7764 (ONLINE)
DOI: 10.29261/pakvetj/2026.251

RESEARCH ARTICLE

Pathological and Transcriptomic Signatures of Tibial Dyschondroplasia and The Therapeutic Potential of Baicalin Via the CDH11/Wnt/β-Catenin Axis

Hemei Yuan[1], Weixing Yang[1], Kaihua Lu[1], Ling Chen[1], Shuqiong Xia[1], Shuang Yang[1], Qian Sun[1], Liu Pan[2], Farid Shokry Ataya[3] and Zhengtian Li[1*]

[1]Yunnan Qujing Normal University, College of Biological and Food Engineering, 655011 Yunnan, China; [2]College of Veterinary Medicine, Huazhong Agricultural University, Wuhan, 430070, China; [3]Department of Biochemistry, College of Science, King Saud University, PO Box 2455, Riyadh 11451, Saudi Arabia.
*Corresponding author: lizhengtian@mail.qjnu.edu.cn

ARTICLE HISTORY (26-1160)

Received: September 26, 2026
Revised: October 23, 2026
Accepted: October 27, 2026
Published online: October 31, 2026

Key words:
Baicalin
Broiler
Cadherin-11
RNA sequencing
Tibial dyschondroplasia
Wnt/β-catenin

ABSTRACT

Tibial dyschondroplasia (TD) is a prevalent skeletal disorder of rapidly growing broilers characterized by an avascular, non-mineralized cartilage plug in the proximal tibiotarsal growth plate and by failure of endochondral ossification; its genome-wide molecular signature and druggable nodes remain incompletely defined. This study integrated histopathology, micro-computed tomography, RNA sequencing and *in-vivo* and *in-vitro* genetic approaches to characterize the TD transcriptome and to determine whether baicalin, a flavone glucuronide from *Scutellaria baicalensis*, ameliorates TD through the cadherin-11 (CDH11)/Wnt/β-catenin axis. One-day-old Arbor Acres broilers (n = 240) were allocated to control (Con), TD, and baicalin (BA) groups; TD and BA birds received 100mg/kg thiram from d 4 to 7 and BA birds received 200mg/kg baicalin from d 8 to 18. TD birds exhibited growth plate thickening, an avascular cartilage plug, proteoglycan depletion, lameness and reduced growth. Baicalin reduced the TD incidence index by 58.4%, normalized growth plate architecture and restored trabecular bone volume. RNA-seq identified 2,847 differentially expressed genes (DEGs) between TD and Con, with gene ontology, KEGG and gene set enrichment analyses converging on suppression of Wnt/β-catenin signaling, chondrocyte differentiation and matrix organization; 66.4% of baicalin-responsive DEGs reverted toward control levels. Quantitative PCR confirmed coordinated suppression of CDH11, WNT3A and CTNNB1 with induction of GSK3B, MMP13, ADAMTS5 and CASP9 in TD, all reversed by baicalin. In primary chondrocytes, baicalin (20μM) reversed thiram-induced loss of viability, apoptosis and cell-cycle arrest; restored β-catenin nuclear translocation and TOPFlash reporter activity; and CDH11 knockdown abolished these effects. These findings identify suppression of CDH11-dependent Wnt/β-catenin signaling as a central molecular signature of TD and demonstrate that baicalin is a therapeutically effective, pathway-targeted intervention within the 18-day experimental period. However, long-term effects on bone mechanical strength, persistence of recovery after treatment withdrawal, and practical dietary safety were not evaluated. Therefore, baicalin should be considered a promising candidate requiring further long-term validation before application in commercial broiler production.

To Cite This Article: Yuan H, Yang W, Lu K, Chen L, Xia S, Yang S, Sun Q, Pan L, Ataya FS and Li Z, 2026. Pathological and transcriptomic signatures of tibial dyschondroplasia and the therapeutic potential of baicalin via the CDH11/Wnt/β-catenin axis. Pak Vet J, 46(10): 2443-2455. http://dx.doi.org/10.29261/pakvetj/2026.251

INTRODUCTION

Tibial dyschondroplasia (TD) is a developmental skeletal disorder of rapidly growing meat-type poultry that originates in the proximal tibiotarsal growth plate and is characterized by the accumulation of an avascular, non-mineralized plug of cartilaginous tissue below the epiphyseal plate, accompanied by growth plate thickening, tibiotarsal deformation, lameness and, in severe cases, fractures and culling (Farquharson and

Jefferies, 2000). The lesion reflects a failure of normal endochondral ossification and compromises both animal welfare and profitability, since affected birds show impaired mobility, reduced feed intake and poor growth and TD remains one of the most frequently diagnosed causes of leg weakness in modern broiler flocks (Rath *et al*., 2004; Shim *et al*., 2012). Because contemporary broilers reach market weight at an ever younger age, the incidence of TD continues to pose a constraint on sustainable intensification of the broiler industry. The etiology of TD is multifactorial, implicating genetic selection for rapid growth and heavy muscling (Shim *et al*., 2012), imbalances in dietary calcium, phosphorus and vitamin D (Leach and Nesheim, 1965; Edwards and Veltmann, 1983) and exposure to mycotoxins and agrochemicals, among which the dithiocarbamate fungicide thiram (tetramethylthiuram disulfide) is the most widely used experimental inducer because it reproducibly produces lesions that are physiologically and pathologically similar to naturally occurring TD (Zhang *et al*., 2018). The thiram-induced model offers several advantages: it induces TD with high regularity and precision, permits precise temporal control of lesion induction and resolution, and reproduces the core histopathological hallmarks of the natural disease, including growth plate thickening, avascular cartilage plug formation, impaired chondrocyte maturation, and failure of endochondral ossification (Kachi *et al*., 2007; Zhang *et al*., 2018). However, the model also has important limitations: it does not replicate the multifactorial etiology of field TD, which involves genetic selection, dietary calcium and phosphorus imbalances, and environmental contributors (Shim *et al*., 2012; Groves and Wilks, 2021); it produces lesions that may be more severe and acute than those of spontaneous TD; and it does not account for the self-healing capacity observed in naturally occurring cases, in which the incidence rate of TD decreases with age (Shi *et al*., 2024). Therefore, findings from this model should be interpreted as mechanistically informative for TD pathogenesis but not as directly generalizable to all forms of naturally occurring TD. Irrespective of the inciting factor, the convergent pathobiology of TD involves disruption of the highly ordered chondrocyte columnar architecture, impaired transition of proliferative chondrocytes to the hypertrophic phenotype, abnormal synthesis and turnover of the cartilage extracellular matrix, disturbed apoptosis and failure of vascular invasion of the hypertrophic zone secondary to aberrant vascular endothelial growth factor signaling (Farquharson and Jefferies, 2000; Jefferies *et al*., 2000; Kronenberg, 2003; Provot and Schipani, 2005; Rath *et al*., 2005). Early molecular studies using subtractive and differential-display approaches identified a set of chondrocyte genes with altered expression in TD cartilage (Jefferies *et al*., 2000; Rath *et al*., 2005), but a comprehensive, system-level description of the TD transcriptome remains lacking. The wingless/integrated (Wnt)/β-catenin signaling cascade is a principal regulator of chondrocyte differentiation, hypertrophy and osteoblastogenesis, and of the cross-talk between these lineages during endochondral bone formation (Hartmann and Tabin, 2001; Akiyama *et al*., 2004; Day *et al*., 2005; Tamamura *et al*., 2005). Aberrant Wnt/β-catenin activity has been linked to a wide spectrum of skeletal diseases (Clevers and Nusse, 2012; Baron and Kneissel, 2013), and because terminal chondrocyte maturation and the switch from cartilage to bone are precisely the processes that fail in TD, this pathway represents a rational candidate for the molecular control of the lesion. Cadherin-11 (CDH11), a classical type II cadherin originally identified as a mesodermally expressed adhesion molecule (Hoffmann and Balling, 1995), mediates cell-cell adhesion in mesenchymal condensations and in fibroblast-like synoviocytes (Valencia *et al*., 2004; Kiener *et al*., 2006; Chang *et al*., 2011). More recently, CDH11 has been shown to govern chondrocyte homeostasis and differentiation by modulating Wnt/β-catenin signaling, with suppression of CDH11 disrupting chondrocyte differentiation through this pathway and contributing to osteoarthritic cartilage damage (Dong *et al*., 2021; Liu *et al*., 2026). Whether CDH11 and its control of Wnt/β-catenin signaling participate in the pathogenesis of TD and whether this axis can be pharmacologically exploited in TD, has not been investigated. RNA sequencing (RNA-seq) provides an unbiased, genome-wide snapshot of the transcriptome that is now routinely applied to uncover disease signatures and drug-responsive pathways in poultry (Yu *et al*., 2012; Dobin *et al*., 2013; Love *et al*., 2014). Coupling RNA-seq with histopathological phenotyping therefore offers a powerful strategy to define the transcriptomic signature of TD, to identify hub pathways such as Wnt/β-catenin, and to resolve the mechanism of action of candidate therapeutics at the pathway level. Baicalin, a flavone glucuronide isolated from the roots of Scutellaria baicalensis Georgi, possesses antioxidant, anti-inflammatory and chondroprotective properties (Li-Weber, 2009) and has recently been shown to ameliorate thiram-induced TD in broiler chickens by suppressing chondrocyte apoptosis and enhancing proliferation through the Bcl-2/caspase-9 and Sox-9/collagen-II systems (Iqbal *et al*., 2023). Nevertheless, the global transcriptional program underlying TD and the ability of baicalin to remodel that program remain unknown. We hypothesized that TD is associated with a characteristic pathological and transcriptomic signature dominated by suppression of the CDH11/Wnt/β-catenin axis, and that baicalin exerts its therapeutic effect by reactivating this axis. Accordingly, the objectives of this study were to (1) characterize the histopathological and transcriptomic signatures of thiram-induced TD in broilers using integrated RNA-seq and histomorphometry; (2) evaluate the therapeutic efficacy of baicalin against established TD; and (3) determine, using in vivo loss- and gain-of-function approaches, whether the CDH11/Wnt/β-catenin axis mediates the chondroprotective effect of baicalin.

MATERIALS AND METHODS

Animals, experimental design and treatments: A total of 240 one-day-old Arbor Acres broiler chicks (40±5g) obtained from a commercial hatchery were randomly allocated to three groups (n=80 per group): control (Con), tibial dyschondroplasia (TD) and baicalin treatment (BA). All birds were housed in electrically heated Petersime-type battery cages under standard management conditions (33–35°C in the first week, thereafter reduced by 2–3°C weekly; 23-h light:1-h dark) and were offered a standard

corn-soybean meal starter diet formulated to meet or exceed the nutrient recommendations of the National Research Council (2001). From day 4 to 7 post-hatch, the TD and BA groups were fed the basal diet supplemented with thiram (tetramethylthiuram disulfide; purity ≥97%) at 100mg/kg feed to induce TD, whereas the Con group received the basal diet only. On day 8, the BA group was switched to the basal diet supplemented with baicalin (purity ≥98%) at 200mg/kg feed administered daily until day 18, while the Con and TD groups continued on the basal diet without additives. Body weight, feed intake, average daily gain, feed conversion ratio and mortality were recorded throughout the 18-day experiment. Lameness was scored daily by two independent observers blinded to treatment using a four-point scale (0 = normal gait; 1 = slight gait abnormality; 2 = obvious lameness with reluctance to walk; 3 = severe lameness, inability to stand) to generate a TD incidence index.

Sample collection and allocation of birds to endpoints: Growth performance, feed intake, mortality and daily lameness scores were obtained from the entire cohort of 80 birds per group. For terminal analyses, subsets of birds were randomly selected and euthanized as follows. On d 10, 14 and 18, six birds per group (n = 6) were weighed and euthanized by cervical dislocation after collection of blood from the wing vein. Serum was separated and stored at −20 °C for biochemical analysis. Both tibiotarsi were excised, trimmed of soft tissue and examined grossly for the presence of the characteristic white, opaque, avascular cartilage plug. Tibia length and mediolateral width, growth plate width and the craniocaudal length of the TD lesion were measured with a digital caliper. The right tibia of each of these birds was fixed in 4 % paraformaldehyde for histology and immunohistochemistry; the left tibia was snap-frozen in liquid nitrogen for subsequent RNA-seq (pooled, see below), quantitative real-time PCR (qRT-PCR) and western blotting (performed on individual or paired samples, n = 6 per group). Additional tibiae from the d-18 subset (n = 6 per group) were used for micro-computed tomography. Proximal growth-plate cartilage was dissected under a stereomicroscope from a further set of birds on d 18 for primary chondrocyte isolation and culture. Thus, all histomorphometric, radiographic, molecular and cell-culture endpoints are based on n = 6 birds per group (or pools derived from those six birds), while growth-performance and clinical-incidence data are based on the full n = 80 birds per group.

Histopathology and histomorphometry: Decalcification of fixed tibial samples was performed using 10% EDTA (pH 7.4) for 30 days with regular changes in the solution. Subsequently, decalcified bones were dehydrated using increasing concentrations of alcohol, cleared in xylene, and embedded in paraffin. Sagittal sections (5μM) from the proximal growth plate were then prepared and stained with hematoxylin-eosin, toluidine blue, and safranin-o fast green. Additional tibiae from d 18 birds (n = 6 per group) were scanned by micro-computed tomography (micro-CT) at 18-μm resolution for three-dimensional reconstruction of the metaphyseal lesion and trabecular bone. Growth plate width, the length of the avascular cartilage plug, and the percentage of trabecular bone volume were quantified in a blinded manner using image-analysis software.

RNA isolation and transcriptome sequencing: RNA was isolated from proximal growth plate cartilage on d 18 using the TRIzol method following the manufacturer's guidelines. Because the amount of pure growth-plate cartilage obtainable from a single 18-day-old broiler is limited, cartilage from six birds per experimental group was pooled to generate each sequencing library. This pooling strategy was adopted solely to obtain sufficient high-quality RNA (RIN > 7.0) for strand-specific library construction while ensuring that every bird within a group contributed equally to the pool. For each experimental group (Con, TD, and BA), cartilage from six birds was pooled to obtain sufficient RNA for library preparation. Thus, one pooled RNA sample was generated per group, and one strand-specific cDNA library was prepared per group (n = 1 pooled library per group; 6 birds per pool; 3 libraries in total). The quality of the RNA was evaluated by electrophoresis on an agarose gel and with the Agilent 2100 Bioanalyzer; samples with an RNA Integrity Number higher than 7.0 were selected. Strand-specific cDNA libraries were prepared with the Illumina TruSeq RNA Sample Preparation kit and then sequenced on the Illumina NovaSeq 6000 platform (150 bp paired-end reads ≥ 20 million reads per library).

Bioinformatics analysis: Raw reads were quality-filtered with fastp (quality score ≥ 30) and aligned to the Gallus gallus reference genome (bGalGal1.mat.broiler.GRCg7b) using STAR (Dobin *et al*., 2013). Gene-level read counts were obtained with featureCounts. Because the RNA-seq design used one pooled library per group without within-group biological replication, DESeq2 could not estimate empirical Bayes dispersion. Therefore, differential expression was assessed using DESeq2 with a fixed dispersion parameter (dispersion = 0.1) and size factors estimated by the median-of-ratios method. The design formula was ~ group. Independent filtering was applied, and P-values were adjusted for multiple testing using the Benjamini–Hochberg method. Genes with |log2 fold-change| ≥ 1 and adjusted $P<0.05$ were considered differentially expressed. Given the absence of biological replication, these adjusted P-values are reported as nominal group-level significance and should be interpreted as exploratory. Hierarchical clustering and principal component analysis were performed on the 500 most variable genes. Gene Ontology (GO) and Kyoto Encyclopedia of Genes and Genomes (KEGG) enrichment analyses of DEGs were conducted with clusterProfiler (Yu *et al*., 2012), and gene set enrichment analysis (GSEA) was applied to rank-ordered gene lists with the Wnt/β-catenin signaling gene set retrieved from the Molecular Signatures Database. Protein–protein interaction networks of DEGs were constructed in STRING and visualized in Cytoscape to identify hub genes, including CDH11.

qRT-PCR validation: Twelve DEGs identified by RNA-seq, including CDH11, WNT3A, β-catenin (CTNNB1), GSK3B, RUNX2, SOX9, COL2A1, ACAN, MMP13, ADAMTS5, VEGFA and CASP9, were validated by

qRT-PCR on an ABI QuantStudio 5 system using SYBR Green master mix with gene-specific primers (Supplementary Table S1) designed with Primer-BLAST; GAPDH served as the internal reference. Relative expression was calculated by the $2^{-\Delta\Delta CT}$ method (Livak and Schmittgen, 2001).

Primary chondrocyte isolation, culture and in vitro treatments. Growth plate chondrocytes were isolated from the proximal tibiotarsi of 14-day-old broilers by enzymatic digestion with 0.25% trypsin for 30 min followed by 0.2% type II collagenase for 4 h at 39°C. Isolated cells were cultured in Dulbecco's modified Eagle's medium/Ham's F-12 (1:1) supplemented with 10% fetal bovine serum and 1% penicillin-streptomycin at 39°C in a 5% CO_2 incubator, and cells at passages 1–2 were used. To establish an in vitro TD model, confluent chondrocytes were challenged with thiram (5μg/mL) for 24h (Zhang *et al*., 2018). To assess the dose-response to baicalin, thiram-challenged cells were treated with baicalin at 0, 10, 20 or 40μM for 24h; 20μM was selected for subsequent experiments.

siRNA knockdown and plasmid transfection: Chondrocytes were transfected with 50nM chicken CDH11-specific small interfering RNA (si-CDH11) or scrambled negative-control siRNA using Lipofectamine 3000, or with a CDH11 overexpression plasmid (pcDNA3.1-CDH11) or empty vector, for 48 h prior to thiram challenge and baicalin treatment. Transfection efficiency was confirmed by qRT-PCR and western blot.

Cell viability, proliferation and apoptosis: The viability of cells was evaluated using the Cell Counting Kit-8. The chondrocyte proliferation was evaluated by EdU uptake and cell-cycle analysis using flow cytometry. Apoptosis was measured by dual staining of annexin V-fluorescein isothiocyanate and propidium iodide as well as TUNEL assay. Activity of alkaline phosphatase in cell lysates was measured with the help of a commercial kit.

TOPFlash/FOPFlash reporter assay. Chondrocytes were cotransfected with TCF/LEF reporter vectors TOPFlash and its control vector FOPFlash and Renilla luciferase plasmid; after the corresponding treatment, the activities of firefly and Renilla luciferases were measured using the Dual-Luciferase Reporter Assay System, and the Wnt/β-catenin transcriptional activity was calculated as TOPFlash/FOPFlash ratio.

Western blot: Chondrocytes of growth plate cartilage were lysed using RIPA buffer supplemented with protease/phosphatase inhibitors at 4°C. Equal amounts of proteins were subjected to SDS-PAGE and then blotted onto PVDF membranes. Immunoblotting was done using primary antibodies for CDH11, Wnt3a, β-catenin (total and dephosphorylated Ser675), phosphorylated GSK3β (Ser9), c-Myc, cyclin D1, Sox9, collagen II, aggrecan, MMP13, ADAMTS5, Bcl-2, Bax, cleaved caspase-9 and β-actin (1:1,000, overnight at 4°C), in addition to secondary HRP-conjugated antibodies

Immunohistochemistry and immunofluorescence: β-catenin and CDH11 distribution in paraffin-embedded growth plate sections was examined by immunohistochemistry with diaminobenzidine detection, and β-catenin nuclear translocation in cultured chondrocytes was visualized by immunofluorescence with 4′,6-diamidino-2-phenylindole counterstaining. Negative controls were incubated with phosphate-buffered saline in place of primary antibody.

Statistical analysis. Data are presented as means±standard error of the mean. Differences among groups were analyzed by one-way analysis of variance followed by Tukey's honestly significant difference test, and TD scores were compared by the Kruskal-Wallis test with Dunn's post-hoc test, using SPSS 26.0 or GraphPad Prism 9. Differences were considered significant at $P<0.05$.

RESULTS

Baicalin ameliorates growth depression and lameness in thiram-challenged broilers: Thiram exposure from d 4 to 7 induced overt TD, with 71.2% of TD-group birds developing gait abnormalities by d 14 and 86.3% by day 18, compared with 0% in the Con group. Baicalin treatment from d 8 onward progressively reduced the incidence and severity of lameness, lowering the TD index by 58.4% relative to the TD group at d 18 ($P<0.001$; Fig. 1). Mortality in the TD group (13.8%) was also significantly higher than in Con (2.5%) and BA (5.0%) birds ($P<0.05$).

Growth performance mirrored the lameness phenotype. Body weight in the TD group diverged from controls beginning at d 10 and remained significantly lower through d 18 (Fig. 1; Table 1). Average daily gain and feed intake were suppressed by 22.7 and 15.3%, respectively, in TD birds, with a corresponding 9.8% deterioration in feed conversion ratio. Baicalin treatment largely restored these parameters: BA birds weighed 16.9% more than TD birds at d 18 ($P<0.01$), with average daily gain, feed intake and feed conversion ratio each returning to levels statistically indistinguishable from the Con group (Table 1). These findings demonstrate that baicalin, administered from d 8 to d 18, reduces the clinical burden of thiram-induced TD and rescues the associated growth failure during the experimental period. Long-term persistence of these benefits after treatment withdrawal was not assessed.

Table 1: Growth performance and mortality of broilers in the Con, TD and BA groups (d 4–18)

Parameter	Con	TD	BA
Body weight at d 18 (g)	674.2±21.3	561.8±24.7c	656.7±22.4d
Average daily gain (g/d, d 8–18)	35.9±1.4	27.7±1.8c	33.2±1.5d
Average daily feed intake (g/d, d 8–18)	48.6±2.1	41.2±2.5c	46.1±2.2d
Feed conversion ratio (d 8–18)	1.35±0.04	1.48±0.06c	1.39±0.05d
Cumulative mortality (%)	2.5	13.8c	5.0d

Values are means±SEM (n = 80 per group). cP<0.01 versus Con; dP<0.05 versus TD.

Baicalin rescues the skeletal phenotype of tibial dyschondroplasia: Gross examination at d 10, 14 and 18 revealed the expected TD lesion—an avascular, white cartilaginous plug below the epiphyseal plate—in all thiram-challenged birds at d 10 and 14, persisting through d 18 in severely affected animals (Fig. 2). Baicalin treatment from d 8 significantly reduced lesion length at

all sampling points, with the greatest therapeutic effect apparent at d 18 (68.2% reduction versus TD; P<0.001; Fig. 2; Table 2). Tibia length, which was shortened by 7.6% in the TD group at d 18, and the widened mediolateral tibial shaft characteristic of the deformity were both normalized by baicalin (Table 2).

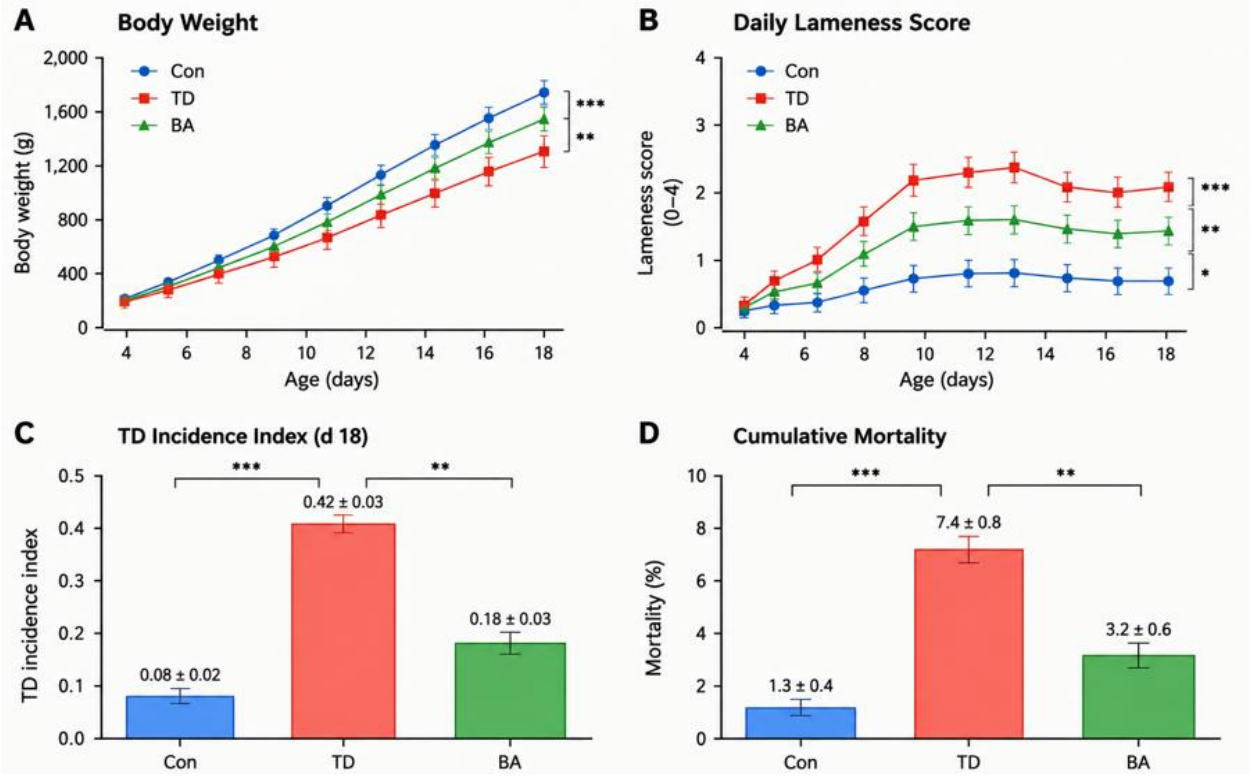


Fig. 1: Effect of baicalin on growth performance and tibial dyschondroplasia (TD) incidence in thiram-challenged broilers. (A) Body weight curves from d 4 to 18 in control (Con), TD and baicalin-treated (BA) groups. (B) Daily lameness scores assessed by the four-point scale described in Materials and Methods. (C) TD incidence index at d 18. (D) Cumulative mortality. Data are means±SEM (n = 80 per group); asterisks denote significant differences versus the TD group (P<0.05, P<0.01, P<0.001).

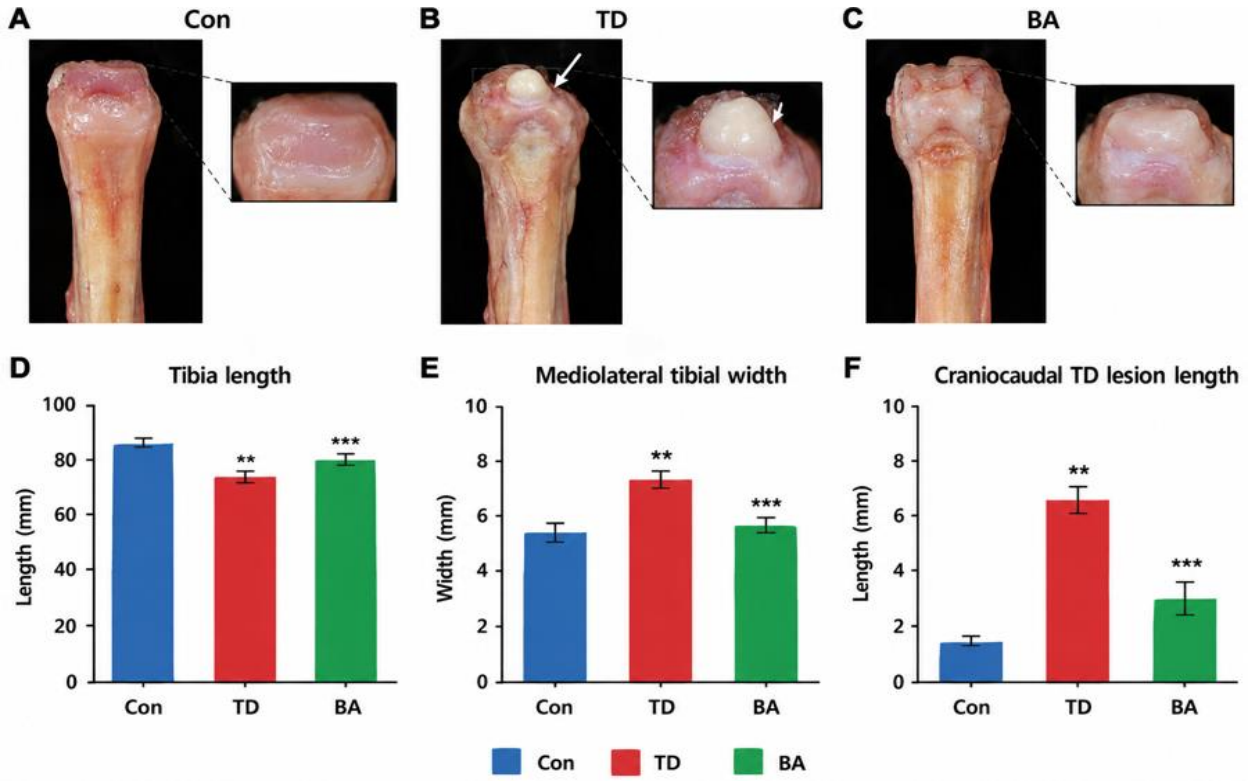


Fig. 2: Gross pathological examination of tibiotarsi at d 18. Representative photographs of the proximal tibiotarsus from Con (A), TD (B) and BA (C) birds. TD birds display the characteristic white, opaque, avascular cartilage plug protruding into the metaphysis (arrow), growth plate thickening and tibiotarsal deformation; baicalin markedly reduces plug size and restores epiphyseal contour. (D–F) Quantification of tibia length, mediolateral tibial width and craniocaudal TD lesion length measured by digital caliper. Data are means±SEM (n = 6 per group per time point); P<0.01, P<0.001 versus TD.

Micro-CT three-dimensional reconstruction confirmed these findings at the tissue level. TD birds showed a persistent metaphyseal radiolucent defect corresponding to the non-mineralized cartilage plug, with markedly reduced trabecular bone volume (BV/TV, −34.5% versus Con; Table 2; Fig. 4). Baicalin restored trabecular architecture, raising BV/TV to 91.2% of control values (P<0.01 versus TD; Table 2).

Histopathology provided the cellular explanation for these macroscopic changes. In Con growth plates, chondrocytes were organized in orderly columns with normal progression from resting, through proliferative, to hypertrophic zones, followed by vascular invasion and endochondral ossification (Fig. 3A, D, G). TD growth plates were thickened by 2.1-fold, showed complete disruption of columnar architecture, an expanded zone of small, non-hypertrophic chondrocytes within the plug, and absence of vascular invasion at the chondro-osseous junction (Fig. 3B, E, H; Table 2). Toluidine blue metachromasia and Safranin O staining were markedly attenuated in TD cartilage, reflecting loss of sulfated proteoglycans from the extracellular matrix. Baicalin treatment restored columnar organization, re-established a recognizable hypertrophic zone with vascular penetration at the plug margin, normalized growth plate width (−47.3% versus TD; Table 2), and recovered strong proteoglycan staining (Fig. 3C, F, I). Together, these data show that baicalin, over the 10-day treatment period (d 8–18), reverses the defining histological features of TD—failed hypertrophic maturation, matrix depletion and absent vascular invasion— at the d 18 endpoint. Whether these improvements persist after baicalin withdrawal and translate into enhanced bone mechanical strength remains to be determined.

Transcriptome profiling defines the molecular signature of TD and its reversal by Baicalin: To obtain a group-level view of the TD transcriptome, we performed RNA-seq on pooled growth plate cartilage (six birds per group; one pooled library per group; three libraries in total). RNA-seq of proximal growth plate cartilage at day 18 generated an average of 24.6 million clean paired-end reads per library (all Q30 ≥ 92.4%), with 91.7% of reads uniquely aligned to the Gallus gallus bGalGal1 mat broiler GRCg7b reference genome. Principal component analysis of the 500 most variable genes separated the three groups cleanly along PC1, which captured 38.6% of total variance; TD samples clustered furthest from Con, with BA samples occupying an intermediate position closer to Con (Fig. 5A). Hierarchical clustering independently confirmed this relationship, demonstrating that baicalin globally remodels the TD transcriptome toward the control state (Fig. 5B).

Table 2: Gross and micro-CT/histomorphometric measurements of the tibiotarsus

Parameter	Time point	Con	TD	BA
Tibia length (mM)	d 18	71.8±1.9	66.3±2.1c	70.2±1.8d
Mediolateral tibial width (mM)	d 18	10.4±0.4	12.9±0.5c	11.1±0.4d
TD lesion length (mM)	d 10 / 14 / 18	— / — / —	6.2±0.5 / 7.8±0.6 / 9.4±0.7	2.4±0.4 / 2.1±0.4 / 3.0±0.5d
Growth plate width (µM)	d 18	612±38	1,296±61c	683±45d
Avascular plug length (µM)	d 18	—	2,847±134c	1,214±112d
Trabecular bone volume (BV/TV, %)	d 18	28.6±2.1	18.7±1.8c	26.1±2.0d

Values are means±SEM (n=6 per group per time point). cP<0.001 versus Con; dP<0.01 versus TD; —, not applicable.

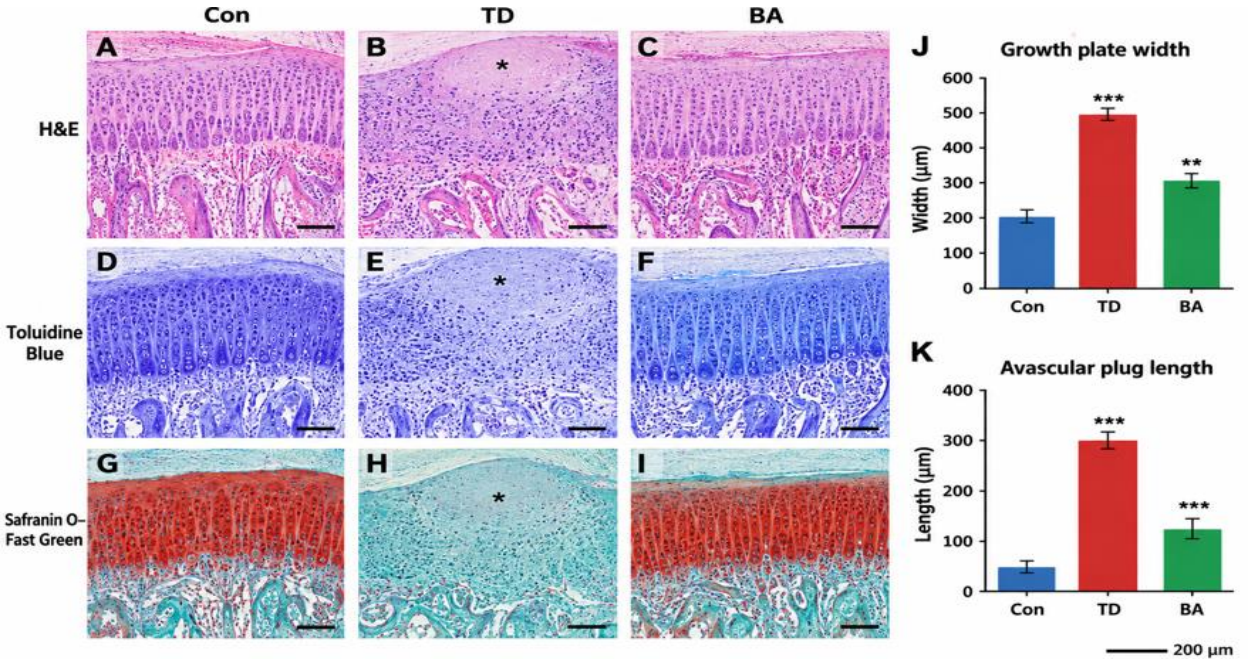


Fig. 3: Histopathological assessment of the proximal tibiotarsal growth plate at d 18. Serial sagittal sections stained with hematoxylin and eosin (A–C), toluidine blue (D–F) and Safranin O–Fast Green (G–I). Con sections show an orderly chondrocyte columnar architecture with an intact hypertrophic zone and vascular invasion (A, D, G). TD sections display a thickened growth plate, loss of chondrocyte columnar organization, accumulation of non-vacuolated resting/proliferative-like chondrocytes, a broad avascular cartilage plug (asterisk) and markedly attenuated Safranin O staining, indicating proteoglycan depletion (B, E, H). BA sections show restored columnar alignment, reappearance of a defined hypertrophic zone, vascular invasion of the plug margin and strong Safranin O staining (C, F, I). (J, K) Blinded histomorphometric quantification of growth plate width and avascular plug length. Data are means±SEM (n = 6 per group); P<0.001 versus Con, P<0.01 and P<0.001 versus TD. Scale bar, 200µM.

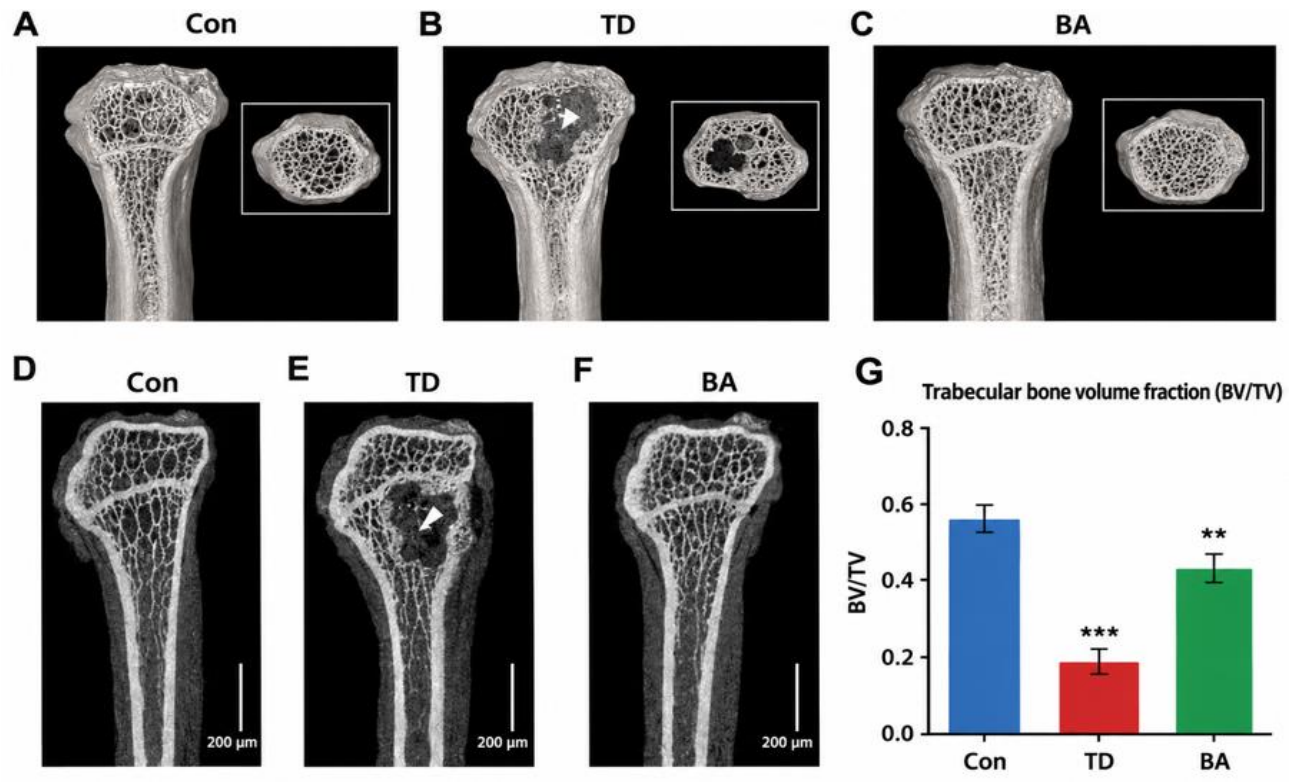


Fig. 4: Micro-computed tomographic analysis of the proximal tibia at d 18. Representative three-dimensional reconstructions (A–C) and sagittal cross-sections (D–F) of Con, TD and BA tibiae. The metaphyseal radiolucent defect in TD birds (arrowhead) is substantially filled with mineralized tissue after baicalin treatment. (G) Quantification of trabecular bone volume fraction (BV/TV). Data are means±SEM (n = 6 per group); P<0.001 versus Con, P<0.01 versus TD.

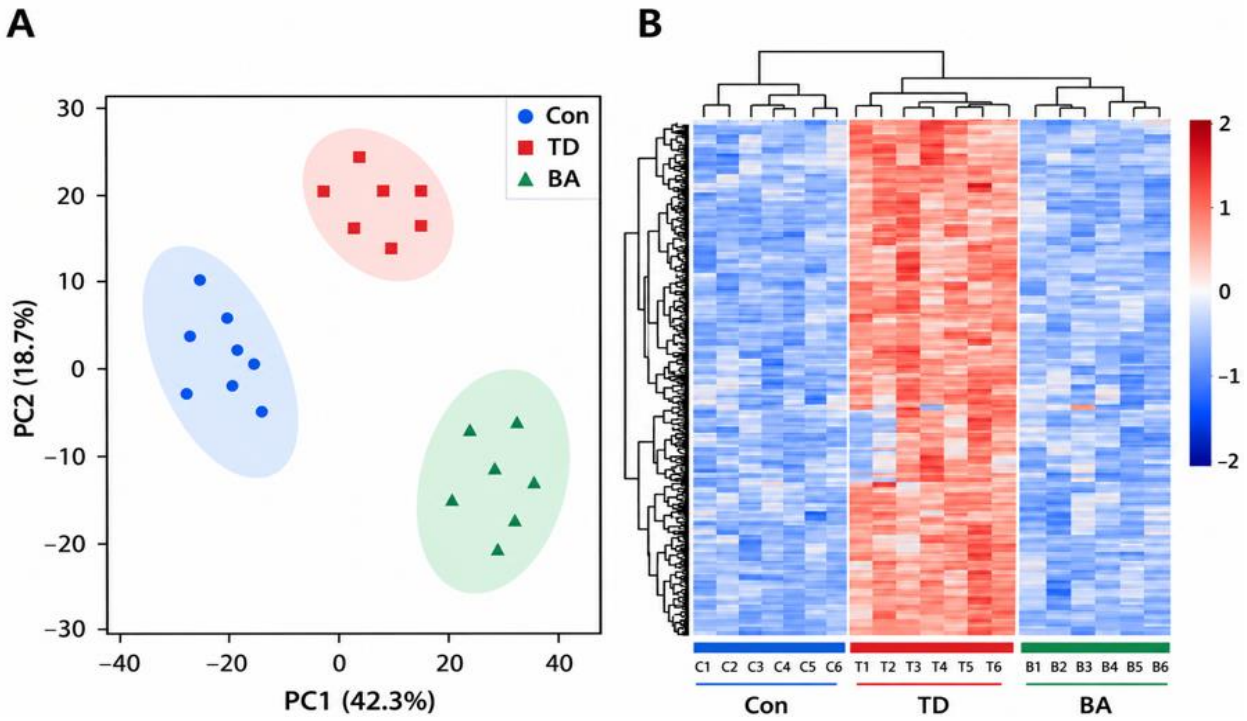


Fig. 5: Transcriptomic signatures of tibial dyschondroplasia and baicalin treatment. (A) Principal component analysis of the 500 most variable genes across Con, TD and BA growth plate libraries (n = 6 pooled birds per group). (B) Hierarchical clustering heat map of differentially expressed genes, showing the BA transcriptome reverting toward the Con state. Color scale represents row-scaled normalized expression (z-score).

A total of 2,847 genes were differentially expressed between TD and Con (|log2 fold-change| ≥ 1, adjusted P<0.05), of which 1,623 were down-regulated and 1,224 up-regulated in TD (Fig. 6A; Table 3). Comparisons of BA versus TD identified 1,914 DEGs (986 up, 928 down; Table 3) and notably, 1,271 genes (66.4% of the BA/TD DEG set) showed expression in BA that reverted toward Con levels in the opposite direction of the TD/Con change (Table 3), indicating that baicalin's therapeutic effect operates largely through reversal of the disease transcriptional program.

Table 3: Summary of differentially expressed genes and pathway-level analyses

Comparison	Total DEGs	Up-regulated	Down-regulated	Genes reverted by treatmenta
TD vs Con	2,847	1,224	1,623	—
BA vs TD	1,914	986	928	1,271 (66.4%)
BA vs Con	412	187	225	—

aGenes altered in TD vs Con whose expression in BA reversed directionally toward Con. Top GO terms among TD-down-regulated genes: chondrocyte differentiation, cartilage development, extracellular matrix organization, endochondral bone morphogenesis. Top KEGG pathways: Wnt signaling, ECM–receptor interaction, PI3K–Akt, focal adhesion. GSEA: Wnt/β-catenin gene set negatively enriched in TD (NES = −2.18, adjusted P<0.001), normalized by baicalin.

GO and KEGG enrichment of the TD-down-regulated genes revealed profound suppression of biological processes integral to endochondral ossification, including "chondrocyte differentiation," "cartilage development," "extracellular matrix organization," "endochondral bone morphogenesis," and "ossification" (Fig. 6B). KEGG analysis ranked the Wnt signaling pathway, "ECM–receptor interaction," "PI3K–Akt signaling" and "focal adhesion" among the most significantly enriched pathways (Fig. 6C). Conversely, TD-up-regulated genes were enriched for apoptotic and catabolic programs, including "regulation of apoptotic process" and "proteolysis" (data not shown). Critically, GSEA of the rank-ordered TD/Con gene list against the Molecular Signatures Database Wnt/β-catenin gene set showed strong negative enrichment in TD (normalized enrichment score = −2.18, adjusted P<0.001), and this enrichment was abolished—returning essentially to the Con level—by baicalin (Fig. 6D). These genome-wide analyses position suppression of Wnt/β-catenin signaling as a central molecular feature of TD and its reactivation as a hallmark of baicalin efficacy.

qRT-PCR validation confirms dysregulation and rescue of the CDH11/Wnt/β-Catenin axis: Twelve DEGs spanning the CDH11/Wnt/β-catenin axis and cartilage homeostasis were validated by qRT-PCR, and all twelve showed directionally concordant changes with the RNA-seq data (Table 4; Pearson r = 0.94 between RNA-seq log2 fold-change and qRT-PCR ΔΔCt values). In TD growth plate, CDH11, WNT3A and CTNNB1 transcripts were suppressed by 61.2, 57.8 and 52.4%, respectively, while the inhibitory kinase GSK3B was up-regulated 2.3-fold, consistent with pathway silencing (Table 4). The catabolic/apoptotic markers MMP13, ADAMTS5 and CASP9 were strongly induced, whereas the anabolic chondrocyte markers SOX9, COL2A1 and ACAN, and the master regulator of hypertrophy RUNX2, were suppressed. Baicalin treatment reversed every one of these changes, restoring CDH11, WNT3A, CTNNB1, RUNX2, SOX9, COL2A1 and ACAN and suppressing GSK3B, MMP13, ADAMTS5 and CASP9 back toward control levels (Table 4).

Table 4: qRT-PCR validation of RNA-seq-identified DEGs in growth plate cartilage at d 18

Gene	TD vs Con (fold-change)	BA vs TD (fold-change)	Direction concordant with RNA-seq
CDH11	0.39±0.05c	2.31±0.24d	Yes
WNT3A	0.42±0.06c	2.18±0.21d	Yes
CTNNB1 (β-catenin)	0.48±0.05c	1.94±0.18d	Yes
GSK3B	2.31±0.19c	0.47±0.06d	Yes
RUNX2	0.52±0.06c	1.88±0.17d	Yes
SOX9	0.44±0.05c	2.05±0.19d	Yes
COL2A1	0.38±0.04c	2.42±0.23d	Yes
ACAN	0.45±0.05c	2.12±0.20d	Yes
MMP13	3.86±0.31c	0.39±0.05d	Yes
ADAMTS5	3.12±0.28c	0.44±0.06d	Yes
VEGFA	0.46±0.05c	1.97±0.18d	Yes
CASP9	3.47±0.29c	0.41±0.05d	Yes

Values are means±SEM (n = 6 per group), expressed as fold-change relative to Con (TD vs Con) or relative to TD (BA vs TD). cP<0.001 versus Con; dP<0.01 versus TD.

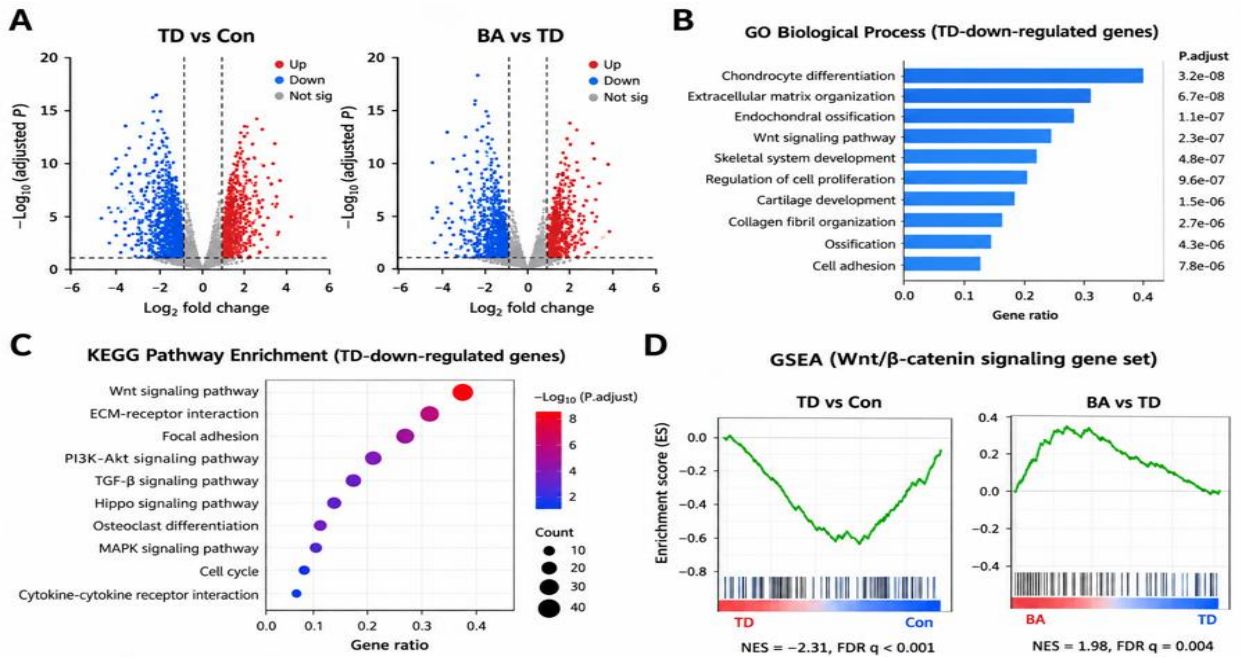


Fig. 6: Differential gene expression and pathway enrichment. (A) Volcano plots of TD versus Con (left) and BA versus TD (right) comparisons; dashed lines indicate |log2 fold-change| = 1 and adjusted P = 0.05. (B) Gene Ontology enrichment (biological process) of TD-down-regulated genes, highlighting terms related to chondrocyte differentiation, extracellular matrix organization, endochondral ossification and Wnt signaling. (C) KEGG pathway enrichment of the same gene set. (D) Gene set enrichment analysis showing significant negative enrichment of the Wnt/β-catenin signaling gene set in TD (normalized enrichment score shown) and its restoration by baicalin.

At the protein level, western blotting of d-18 growth plate tissue mirrored the transcript data: CDH11, Wnt3a, total and non-phospho (Ser675) β-catenin, phospho-GSK3β (Ser9), c-Myc and cyclin D1 were all markedly reduced in TD and restored by baicalin (Fig. 7A, B). Sox9, collagen II and aggrecan protein abundance was similarly depressed in TD and rescued by BA, while MMP13, ADAMTS5 and Bax were induced and cleaved caspase-9 was elevated in TD, with each normalized by baicalin; anti-apoptotic Bcl-2 showed the reciprocal pattern (Fig. 7A, B). Immunohistochemistry localized this effect spatially: β-catenin and CDH11 immunoreactivity was abundant throughout the growth plate in Con birds, markedly attenuated within the TD cartilage plug, and restored in BA birds (Fig. 7C, D). Together, these data validate the RNA-seq findings and identify coordinated suppression—followed by baicalin-mediated reactivation—of the CDH11/Wnt/β-catenin axis as a defining molecular event in TD pathogenesis and treatment.

Baicalin protects primary chondrocytes against thiram injury through CDH11-dependent Wnt/β-catenin signaling: To test causality, we established an *in-vitro* TD model in which thiram (5μg/mL, 24 h) reduced primary chondrocyte viability by 42.8% and increased the apoptotic fraction from 8.4 to 39.7% (annexin V/PI; Fig. 8A, C). Baicalin dose-dependently rescued viability (EC50 ≈ 18μM), with 20μM restoring viability to 91.3% of control; this concentration was used for all subsequent experiments. EdU incorporation and cell-cycle analysis showed that thiram arrested chondrocytes in G0/G1 and suppressed proliferation by 54.1%, effects that 20μM baicalin reversed (EdU-positive cells restored to 88.7% of control; Fig. 8B). TUNEL staining and flow cytometry confirmed parallel suppression of thiram-induced apoptosis (from 39.7 to 14.2%; Fig. 8C). Thiram also suppressed alkaline phosphatase activity by 58.6%, indicating impaired maturation; baicalin restored it to 92.4% of control. At the molecular level, thiram suppressed CDH11, Wnt3a, β-catenin (total and Ser675) and phospho-GSK3β, whereas baicalin restored them (Fig. 8D). TOPFlash/FOPFlash reporter assays showed that thiram reduced Wnt/β-catenin transcriptional activity by 63.5%, an effect fully reversed by baicalin, and immunofluorescence confirmed that baicalin restored β-catenin nuclear translocation, which was abolished by thiram challenge.

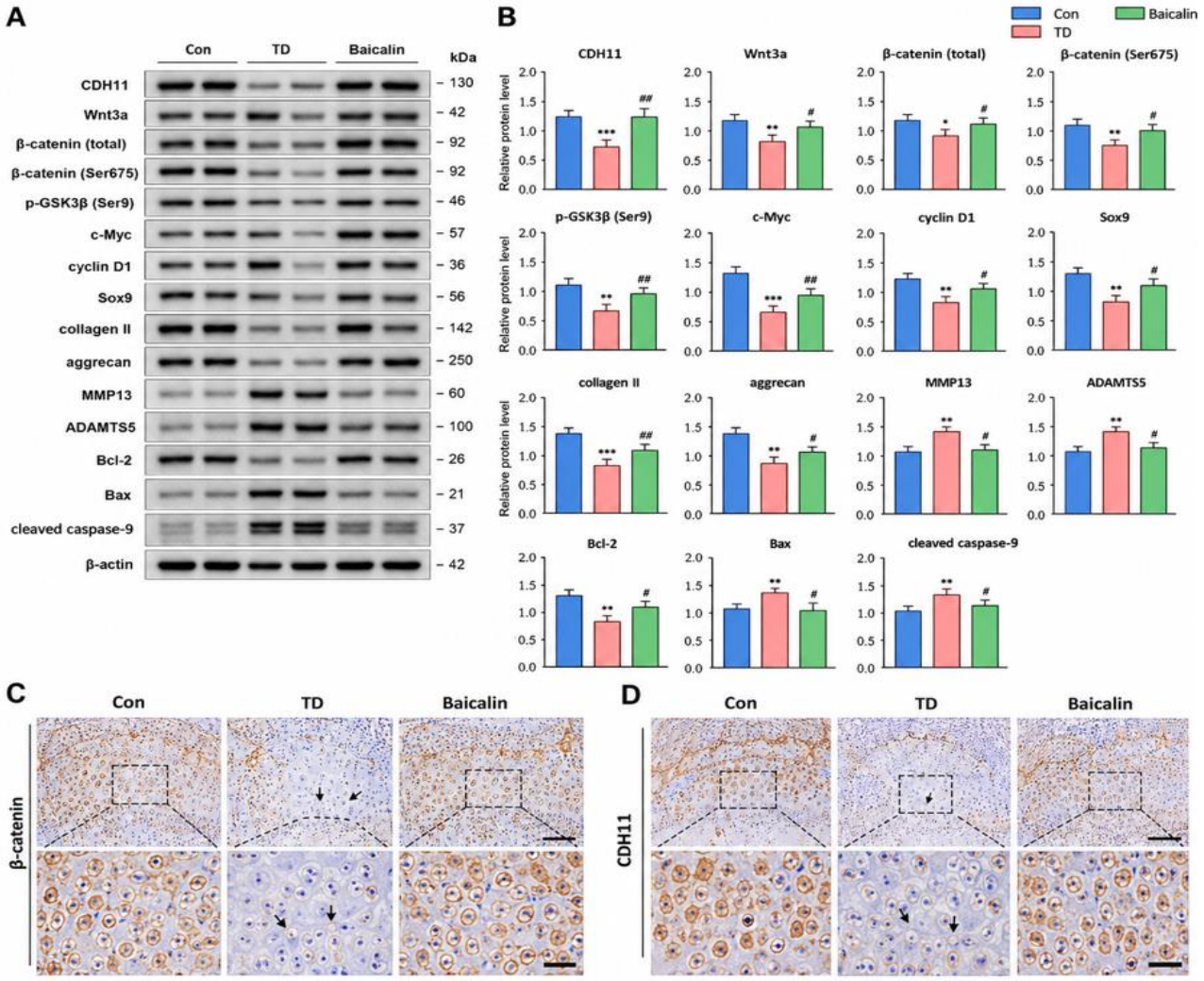


Fig. 7: *In-vivo* evidence for baicalin-mediated reactivation of the CDH11/Wnt/β-catenin axis in the growth plate. (A) Representative western blots of d-18 growth plate lysates probed for CDH11, Wnt3a, total and non-phospho β-catenin (Ser675), phospho-GSK3β (Ser9), c-Myc, cyclin D1, Sox9, collagen II, aggrecan, MMP13, ADAMTS5, Bcl-2, Bax, cleaved caspase-9 and β-actin. (B) Densitometric quantification normalized to β-actin. (C, D) Immunohistochemical staining of β-catenin and CDH11 in proximal growth plate sections; arrows indicate attenuated staining within the TD cartilage plug and restored signal after baicalin. Data are means±SEM (n = 6 per group); P<0.05, P<0.01, P<0.001 versus TD; #P<0.05, ##P<0.01 versus Con. Scale bar, 100μM.

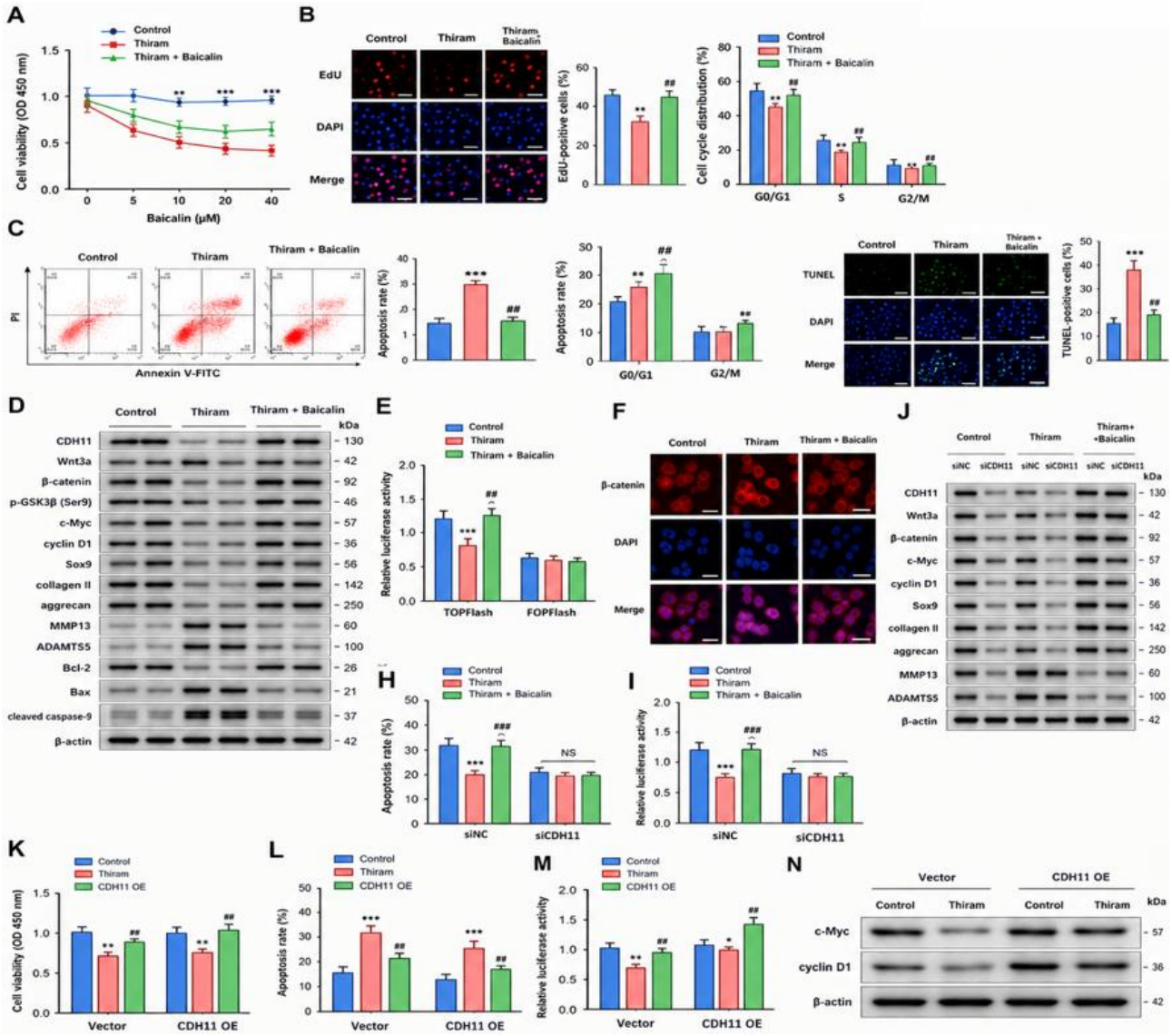


Fig. 8: The CDH11/Wnt/β-catenin axis mediates the chondroprotective effect of baicalin *in-vitro*. (A) Cell viability (CCK-8) of thiram-challenged chondrocytes treated with increasing baicalin concentrations (0–40μM). (B) EdU incorporation and cell-cycle distribution. (C) Annexin V/PI flow-cytometric quantification and representative TUNEL staining of apoptosis. (D) Western blotting of CDH11, Wnt3a, β-catenin, phospho-GSK3β (Ser9), c-Myc, cyclin D1, Sox9, collagen II, aggrecan, MMP13, ADAMTS5, Bcl-2, Bax, cleaved caspase-9 and β-actin. (E) TOPFlash/FOPFlash luciferase reporter assay of Wnt/β-catenin transcriptional activity. (F) Immunofluorescence of β-catenin nuclear translocation (4′,6-diamidino-2-phenylindole counterstain). (G–J) Loss-of-function: siRNA-mediated CDH11 knockdown (verified by qRT-PCR and western blot) abolishes baicalin's rescue of viability (G), apoptosis (H), TOPFlash activity (I) and anabolic marker expression (J) in thiram-challenged cells. (K–N) Gain-of-function: CDH11 overexpression (pcDNA3.1-CDH11) phenocopies baicalin, restoring viability (K), reducing apoptosis (L), activating TOPFlash (M) and inducing c-Myc/cyclin D1 (N). Data are means±SEM of three independent experiments; P<0.05, P<0.01, P<0.001 versus the thiram-alone group; NS, not significant.

Mechanistically, siRNA knockdown of CDH11 (efficiency 78.4% at mRNA and 74.1% at protein level) abolished the ability of baicalin to rescue viability, suppress apoptosis, restore TOPFlash activity or induce Sox9/collagen II/aggrecan in thiram-challenged chondrocytes (Fig. 8G–J). Conversely, CDH11 overexpression phenocopied baicalin in the absence of the drug: pcDNA3.1-CDH11 transfection restored viability to 89.6% of control, reduced the apoptotic fraction to 16.8%, reactivated TOPFlash/FOPFlash signaling and induced c-Myc, cyclin D1 and the cartilage matrix program (Fig. 8K–N). Neither scrambled siRNA nor empty vector altered any measured endpoint. These gain- and loss-of-function experiments establish that the chondroprotective effect of baicalin in vitro is mediated specifically through CDH11-dependent reactivation of Wnt/β-catenin signaling, rather than through parallel antioxidant or anti-inflammatory mechanisms alone. However, these experiments do not establish a direct physical interaction between CDH11 and β-catenin, nor do they address long-term outcomes *in-vivo*.

DISCUSSION

In this study, we combined gross pathology, histomorphometry, micro-computed tomography, RNA sequencing, and in vivo and in vitro genetic gain- and loss-of-function experiments to characterize the pathological and transcriptomic signature of thiram-induced tibial dyschondroplasia (TD) and to define the mechanism by which baicalin ameliorates the lesion. Our principal findings are fourfold. First, thiram-induced TD in broilers reproduced the full clinical and pathological spectrum of the natural disease lameness, growth plate thickening, an

avascular non-mineralized cartilage plug, proteoglycan depletion, failed hypertrophic maturation, and suppressed growth validating the model. Second, transcriptome profiling revealed that TD is a transcriptionally coherent disease dominated by suppression of chondrocyte differentiation, extracellular matrix organization and Wnt/β-catenin signaling. Third, baicalin, administered after lesion induction, substantially reversed the clinical, histological, radiographic and molecular phenotype of established TD, and approximately two-thirds of the baicalin-responsive transcriptome reverted toward the control state. Fourth, and most importantly, the chondroprotective effect of baicalin was abolished by CDH11 knockdown and phenocopied by CDH11 overexpression, establishing the CDH11/Wnt/β-catenin axis as a causal mediator rather than a bystander marker of baicalin action. The histological features observed in the TD group—a thickened growth plate, accumulation of small non-hypertrophic chondrocytes within the plug, loss of columnar architecture, attenuated toluidine blue metachromasia and Safranin O staining, and absence of vascular invasion at the chondro-osseous junction—closely mirror descriptions of spontaneous and experimentally induced TD (Farquharson and Jefferies, 2000; Jefferies *et al*., 2000). The lesion is widely regarded as a failure of proliferative chondrocytes to execute the hypertrophic program and of the hypertrophic cartilage to undergo vascular invasion and endochondral replacement, processes orchestrated by the ordered interplay of Sox9, Runx2, vascular endothelial growth factor and Wnt signals (Kronenberg, 2003; Provot and Schipani, 2005; Zhang *et al*., 2018). Our finding that baicalin restored a defined hypertrophic zone, vascular penetration of the plug margin, proteoglycan content and trabecular bone volume indicates that baicalin acts on the fundamental maturation defect of TD rather than merely masking clinical signs—a distinction of considerable importance, because agents that relieve lameness without restoring endochondral ossification would be expected to leave birds with structurally compromised bone (Rath *et al*., 2004; Shim *et al*., 2012). A central contribution of this study is the genome-wide definition of the TD transcriptome. The 2,847 differentially expressed genes identified between TD and control growth plate cartilage, and their enrichment for terms including chondrocyte differentiation, cartilage development, extracellular matrix organization and endochondral ossification, provide a systems-level confirmation of what histopathology had long implied: TD is, at its core, a disease of arrested chondrocyte maturation and matrix failure. Gene set enrichment analysis specifically implicated suppression of Wnt/β-catenin signaling, consistent with the established role of this pathway in coordinating the transition from proliferative to hypertrophic chondrocytes and the chondrocyte-to-osteoblast lineage switch (Akiyama *et al*., 2004; Day *et al*., 2005; Tamamura *et al*., 2005). Canonical Wnt signaling must be precisely titrated during endochondral ossification—excessive activity can suppress chondrogenesis, whereas insufficient activity impairs osteoblastogenesis and hypertrophic transition (Yang *et al*., 2003; Hill *et al*., 2005). Our data place thiram-induced TD firmly on the hypo-Wnt side of this balance, with reduced WNT3A and β-catenin expression, increased inhibitory GSK3B, reduced non-phospho β-catenin (Ser675) and reduced target gene output (c-Myc, cyclin D1), together with reciprocal induction of the catabolic and apoptotic machinery (MMP13, ADAMTS5, CASP9) and suppression of anabolic markers (SOX9, COL2A1, ACAN). That baicalin restored each of these parameters, and that 66.4% of baicalin-responsive DEGs reverted directionally toward control levels, indicates that the drug acts on the disease program itself and not on an orthogonal pathway. CDH11 emerged from protein-protein interaction network analysis as a hub gene, and its expression pattern—suppressed in TD, restored by baicalin—positioned it as a candidate upstream regulator. CDH11 is a classical type II cadherin expressed in mesenchymal condensations, where it mediates the cell-cell adhesion required for tissue patterning during skeletogenesis (Hoffmann and Balling, 1995; Valencia *et al*., 2004; Kiener *et al*., 2006; Chang *et al*., 2011). More recent work has shown that CDH11 governs chondrocyte homeostasis by modulating Wnt/β-catenin signaling, with CDH11 suppression disrupting chondrocyte differentiation and contributing to osteoarthritic cartilage damage (Dong *et al*., 2021; Liu *et al*., 2026). Our data extend this axis to TD and, critically, add causal evidence from a non-mammalian growth-plate system: siRNA-mediated CDH11 knockdown abolished baicalin's rescue of viability, apoptosis, Wnt/β-catenin transcriptional activity and anabolic gene expression, whereas CDH11 overexpression reproduced the therapeutic phenotype in the absence of the drug. Because neither manipulation affected outcomes in the absence of thiram challenge, we interpret CDH11 as a stress-responsive gatekeeper: thiram suppresses CDH11, thereby silencing Wnt/β-catenin output and locking chondrocytes in an immature, apoptosis-prone state; baicalin releases this block by restoring CDH11 expression and function. Our findings are consistent with, and substantially extend, the report of Iqbal *et al*. (2023) that baicalin ameliorates thiram-induced TD in broilers by suppressing chondrocyte apoptosis and enhancing proliferation through the Bcl-2/caspase-9 and Sox-9/collagen-II systems. We confirmed each of those molecular readouts in the present dataset, but the transcriptomic and genetic approaches used here allow a mechanistic synthesis: baicalin-mediated restoration of CDH11 and Wnt/β-catenin signaling provides a plausible upstream explanation for the downstream normalization of Bcl-2/Bax/caspase-9 and Sox9/collagen-II/aggrecan, since Wnt/β-catenin target genes such as cyclin D1 and c-Myc regulate proliferation and survival, and since Wnt and Sox9 pathways are known to antagonize and balance one another during chondrocyte fate decisions (Akiyama *et al*., 2004). Baicalin's antioxidant and anti-inflammatory properties have been documented in many systems (Li-Weber, 2009), and we cannot exclude contributing parallel or upstream effects that converge on the CDH11/Wnt/β-catenin axis. However, the complete abrogation of baicalin's rescue of viability, apoptosis, and Wnt/β-catenin transcriptional activity by CDH11 knockdown indicates that CDH11 is functionally required for these specific chondroprotective endpoints in our in vitro model, even if additional CDH11-independent mechanisms may contribute to other aspects of baicalin's activity. From an applied perspective, these results support dietary baicalin as a promising candidate intervention for TD in commercial broiler flocks, where leg

disorders compromise welfare, growth and carcass value and remain among the most frequent reasons for culling (Rath *et al*., 2004; Shim *et al*., 2012). The post-induction treatment schedule used here—baicalin beginning on d 8, after thiram withdrawal—models therapeutic rather than purely prophylactic use within the 18-day study period. However, several important questions remain unanswered: (1) whether the therapeutic benefits persist after baicalin withdrawal; (2) whether restored growth plate architecture translates into improved bone mechanical strength; (3) whether longer-term baicalin administration is safe and free of adverse effects on liver, kidney, or other organ systems; and (4) whether baicalin is effective in naturally occurring TD, which has a multifactorial etiology and a potentially self-limiting course. Consequently, our findings interpreted as defining a molecular mechanism of TD pathogenesis under controlled experimental conditions, and the translational potential of baicalin should be evaluated in naturally occurring TD before conclusions about commercial efficacy can be drawn. There are a few limitations of this study, including: the RNA-seq libraries were constructed from pooled cartilage (six birds per group) to achieve adequate RNA yield from the limited quantity of pure proximal growth-plate tissue available from individual 18-day-old broilers. While this approach enabled robust detection of the dominant disease transcriptome and its reversal by baicalin, it precludes formal biological replication at the individual-animal level and therefore limits statistical inference of inter-animal heterogeneity. Consequently, the DEGs reported here represent group-level consensus signatures rather than animal-specific expression profiles. Future studies employing low-input or single-nucleus RNA-seq on individual growth plates will be required to resolve cell-type-specific and inter-bird variation within the TD signature. Second, although loss- and gain-of-function experiments establish necessity and sufficiency of CDH11 in vitro, the direct physical or transcriptional mechanism by which baicalin upregulates CDH11—whether through promoter-level effects, microRNA regulation as suggested for miR-127-3p and miR-205a (Dong *et al*., 2021; Liu *et al*., 2026), or relief of oxidative repression—remains to be defined. Third, the study was conducted using a thiram-induced model of TD, which reproduces the core histopathological features of spontaneous TD but does not capture the multifactorial etiology, chronic progression, or self-healing potential of naturally occurring TD. Therefore, the efficacy of baicalin observed here requires validation in naturally occurring TD and in field trials before conclusions about commercial efficacy can be drawn. Fourth, although our gain- and loss-of-function experiments establish CDH11 as functionally required for baicalin's rescue of viability, apoptosis, and Wnt/β-catenin transcriptional activity in vitro, the study was not designed to systematically dissect CDH11-dependent versus CDH11-independent effects. Baicalin possesses well-documented antioxidant (Nrf2/HO-1), anti-inflammatory (NF-κB), and anti-ferroptotic activities that were not directly measured in this study (Li-Weber, 2009). Consequently, we cannot exclude the possibility that baicalin exerts additional chondroprotective effects through CDH11-independent mechanisms, or that antioxidant and anti-inflammatory actions converge on and support the CDH11/Wnt/β-catenin axis. Future studies should incorporate oxidative stress and inflammatory marker profiling, Nrf2 and NF-κB pathway manipulation, and combinatorial pathway blockade to define the relative contributions of these mechanisms.

Conclusions: Thiram-induced tibial dyschondroplasia in broilers is characterized by a coherent transcriptomic signature dominated by suppression of chondrocyte differentiation, extracellular matrix organization and Wnt/β-catenin signaling, together with induction of apoptosis and matrix catabolism. Baicalin administered after lesion induction substantially reverses the clinical, histological, radiographic and molecular phenotype of established TD. Gain- and loss-of-function experiments in primary chondrocytes demonstrate that the CDH11/Wnt/β-catenin axis is necessary and sufficient for baicalin's chondrotective effect, identifying this axis as a central druggable node in TD pathogenesis. However, several critical questions remain unanswered. The long-term persistence of recovery after baicalin withdrawal, the effects of baicalin on bone mechanical strength, and the practical dietary safety of baicalin were not evaluated. Furthermore, the efficacy of baicalin in naturally occurring TD, which has a multifactorial etiology and a potentially self-limiting course, remains to be established. Therefore, baicalin should be considered a promising, mechanistically defined, pathway-targeted candidate for the control of TD that warrants further long-term evaluation, including mechanical testing, safety assessment, and field trials, before application in commercial broiler production. Direct molecular interaction between CDH11 and Wnt/β-catenin pathway components also remains to be established in future work.

Data availability statement: All data generated or used during this study are included in this article.

Conflict of interest statement: Authors declared no competing interest.

Ethics statement: All animal procedures were approved by Animal Care and Use Committee (SYXK-2026-057) in accordance with the guidelines of the National Research Council Guide for the Care and Use of Laboratory Animals (National Research Council, 2011) and the European Union Directive 2010/63/EU on the protection of animals used for scientific purposes. Birds were monitored twice daily for welfare indicators including feed and water intake, mobility, respiratory distress, and mortality, and were humanely euthanised by cervical dislocation at predetermined endpoints.

Funding: Supported by the Special Program for Building a South and Southeast Asia-Focused Center for Science and Technology Innovation (202403AK140028). The authors extend their appreciation to “Ongoing Research Funding Program" (ORF-2026-693), King Saud University, Riyadh, Saudi Arabia.

Authors contribution: HY and ZL conceptualized and designed the study. HY, WY, KL and LC performed the animzal experiments, including thiram induction of tibial dyschondroplasia, baicalin treatment, growth-performance

recording, lameness scoring and tissue collection. SX, SY, FSA, LP and QS conducted molecular, histological and biochemical assays, including RNA sequencing, qRT-PCR, western blotting, immunohistochemistry, immunofluorescence, TUNEL, CCK-8, EdU, flow cytometry, TOPFlash/FOPFlash reporter assays, and primary chondrocyte culture with siRNA knockdown and overexpression. HY, WY, FSA and LP performed statistical analysis and data visualization. HY drafted the original manuscript. ZL supervised the project, acquired funding and critically revised the manuscript. All authors contributed to data interpretation, reviewed and edited the manuscript, and approved the final version.

Acknowledgments: This research is supported by the Special Program for Building a South and Southeast Asia-Focused Center for Science and Technology Innovation (202403AK140028). The authors extend their appreciation to "Ongoing Research Funding Program" (ORF-2026-693), King Saud University, Riyadh, Saudi Arabia.

REFERENCES

Akiyama H, Lyons JP, Mori-Akiyama Y, *et al*., 2004. Interactions between Sox9 and beta-catenin control chondrocyte differentiation. Genes and Development 18:1072-1087. https://doi.org/10.1101/gad.1178704

Baron R and Kneissel M, 2013. WNT signaling in bone homeostasis and disease: from human mutations to treatments. Nature Medicine 19:179-192. https://doi.org/10.1038/nm.3074

Chang SK, Gu Z, Litvin J, *et al*., 2011. Cadherin-11 regulates fibroblast inflammation. Proceedings of National Academy of Science 108:8402-8407. https://doi.org/10.1073/pnas.1019382108

Clevers H and Nusse R, 2012. Wnt/beta-catenin signaling and disease. Cell 149:1192-1205. https://doi.org/10.1016/j.cell.2012.05.012

Day TF, Guo X, Garrett-Beal L, *et al*., 2005. Wnt/beta-catenin signaling in mesenchymal progenitors controls osteoblast and chondrocyte differentiation during vertebrate skeletogenesis. Developmetal Cell 8:739-750. https://doi.org/10.1016/j.devcel.2005.02.022

Dobin A, Davis CA, Schlesinger F, *et al*., 2013. STAR: ultrafast universal RNA-seq aligner. Bioinformatics 29:15-21. https://doi.org/10.1093/bioinformatics/bts635

Dong J, Wang Z, Zhou L, *et al*., 2021. Exosome-encapsulated microRNA-127-3p released from bone marrow-derived mesenchymal stem cells alleviates osteoarthritis by targeting CDH11 to block the Wnt/beta-catenin pathway. Journal of Pain Research14:2187-2202. https://doi.org/10.2147/JPR.S309078

Edwards HM and Veltmann JR, 1983. The role of calcium and phosphorus in the etiology of tibiotarsal dyschondroplasia in young chicks. Journal of Nutrition 113:1568-1575. https://doi.org/10.1093/jn/113.8.1568

Farquharson C and Jefferies D, 2000. Chondrocytes and longitudinal bone growth: the development of tibiotarsal dyschondroplasia. Poultry Science 79:994-1004. https://doi.org/10.1093/ps/79.7.994

Hartmann C and Tabin CJ, 2001. Wnt-14 plays a pivotal role in inducing synovial joint formation in the developing appendicular skeleton. Cell 104:341-351. https://doi.org/10.1016/S0092-8674(01)00231-7

Hill TP, Später D, Taketo MM, *et al*., 2005. Canonical Wnt/beta-catenin signaling prevents osteoblasts from differentiating into chondrocytes. Developmetal Cell 8:727-738. https://doi.org/10.1016/j.devcel.2005.02.013

Hoffmann I and Balling R, 1995. Cloning and expression analysis of a novel mesodermally expressed cadherin. Developmetal Biology 169:337-346. https://doi.org/10.1006/dbio.1995.1151

Iqbal M, Waqas M, Mo Q, *et al*., 2023. Baicalin inhibits apoptosis and enhances chondrocyte proliferation in thiram-induced tibial dyschondroplasia in chickens by regulating Bcl-2/Caspase-9 and Sox-9/collagen-II expressions. Ecotoxicology and Environmental Safety 268:115689. https://doi.org/10.1016/j.ecoenv.2023.115689

Jefferies D, Houston B, Lester D, *et al*., 2000. Expression patterns of chondrocyte genes cloned by differential display in tibiotarsal dyschondroplasia. Biochimstry and Biophysics Acta 1501:180-188. https://doi.org/10.1016/S0925-4439(00)00029-0

Kachi M, Sugiyama T and Kusuhara S, *et al*., 2007. Morphological observations of induced lesions of tibial dyschondroplasia in broiler chicken. Animal Science Journal, 78: 187–193.

Kiener HP, Lee DM, Agarwal SK, *et al*., 2006. Cadherin 11 promotes invasive behavior of fibroblast-like synoviocytes. Arthritis Rheumitis 54:726-732. https://doi.org/10.1002/art.21665

Kronenberg HM, 2003. Developmental regulation of the growth plate. Nature 423:332-336. https://doi.org/10.1038/nature01657

Leach RM and Nesheim MC, 1965. Studies on tibial dyschondroplasia in chickens. Journal of Nutrition 86:236-242. https://doi.org/10.1093/jn/86.3.236

Li-Weber M, 2009. New therapeutic aspects of flavones: the anticancer properties of Scutellaria and its main active constituents wogonin, baicalein and baicalin. Cancer Treatment Reviews 35:57-68. https://doi.org/10.1016/j.ctrv.2008.09.005

Liu K, Zhang Y, Wang X, *et al*., 2026. miR-205a-mediated suppression of CDH11 disrupts Wnt/β-catenin signaling in chondrocytes. Cell Death Discovery 12:185. https://doi.org/10.1038/s41420-026-03146-3

Livak KJ and Schmittgen TD, 2001. Analysis of relative gene expression data using real-time quantitative PCR and the 2(-Delta Delta C(T)) method. Methods 25:402-408. https://doi.org/10.1006/meth.2001.1262

Love MI, Huber W and Anders S, 2014. Moderated estimation of fold change and dispersion for RNA-seq data with DESeq2. Genome Biology 15:550. https://doi.org/10.1186/s13059-014-0550-8

National Research Council, 2001. Nutrient requirements of poultry. 9th revised. edn. National Academy Press, Washington, DC.

Provot S and Schipani E, 2005. Molecular mechanisms of endochondral bone development. Biochemistry and Biophysics Research Communications 328:658-665. https://doi.org/10.1016/j.bbrc.2004.11.148

Rath NC, Anthony NB, Kannan L, *et al*., 2005. Serum proteomic profiles of broiler chickens with tibiotarsal dyschondroplasia. Poultry Science 84:725-732. https://doi.org/10.1093/ps/84.5.725

Rath NC, Huff GR, Huff WE, *et al*., 2004. Factors regulating bone maturity and strength in poultry. Poultry Science 83:1060-1072. https://doi.org/10.1093/ps/83.7.1060

Shi K, Wu Y, Jiang X, *et al*., 2024. Transcriptome analysis reveals the pathogenesis of spontaneous tibial dyschondroplasia in broilers. Frontiers in Genetics, 15: 1434532

Shim MY, Karnuah AB, Mitchell AD, *et al*., 2012. The effects of growth rate on leg morphology and tibiotarsal breaking strength, mineral density, mineral content, and bone ash in broilers. Poultry Science 91:1790-1795. https://doi.org/10.3382/ps.2011-01981

Tamamura Y, Otani T, Kanatani N, *et al*., 2005. Developmental regulation of Wnt/beta-catenin signals is required for growth plate assembly, cartilage integrity, and endochondral ossification. Journal of Biology and Chemistry 280:19185-19195. https://doi.org/10.1074/jbc.M500558200

Valencia JW, Kiener HP, Agarwal SK, *et al*., 2004. Cadherin-11 provides specific cellular adhesion between fibroblast-like synoviocytes. Journal of Experimental Medicine 200:1673-1679. https://doi.org/10.1084/jem.20041043

Yang Y, Topol L, Lee H, *et al*., 2003. Wnt5a and Wnt5b exhibit distinct activities in coordinating chondrocyte proliferation and differentiation. Development 130:1003-1015. https://doi.org/10.1242/dev.00324

Yu G, Wang LG, Han Y, *et al*., 2012. Clusterprofiler: an R package for comparing biological themes among gene clusters. OMICS 16:284-287. https://doi.org/10.1089/omi.2011.0118

Zhang H, Shao Y, Zeng X, *et al*., 2018. Icariin ameliorate thiram-induced tibial dyschondroplasia via regulation of WNT4 and VEGF expression in broiler chickens. Frontiers in Pharmacology 9:1432. https://doi.org/10.3389/fphar.2018.01432